

A FUSION STRATEGY FOR EXTRACTED ROAD NETWORKS FROM MULTI-ASPECT SAR IMAGES

K. Hedman, B. Wessel, U. Stilla

Photogrammetry and Remote Sensing, Technische Universitaet Muenchen,
Arcisstrasse 21, 80333 Muenchen, Germany

{karin.hedman,birgit.wessel,stilla}@bv.tum.de

KEY WORDS: SAR, road extraction, multi-aspect images, fusion

ABSTRACT:

In this paper, we describe an extension of the automatic road extraction procedure developed for single SAR images towards multi-aspect SAR images. Multi-aspect images illuminate the same scene, but from different directions. For the combination of the extracted information, a fusion technique is introduced. Each road segment is assessed according to its direction compared to the direction of the illumination. Due to the side-looking geometry of SAR, the visibility of roads is often limited by adjacent trees or building rows. Roads in viewing direction are less affected by shadow and layover effects from neighbouring objects than roads across the viewing direction. Road segments are evaluated, according to its expected visibility. Roads in viewing direction are therefore higher evaluated, than roads running in azimuth direction. The fusion technique is demonstrated on two sub-urban SAR scenes. The results show the potential of the proposed fusion strategy; with the use of two or more views, the resulting road network is more complete and more correct than for each single image.

1. INTRODUCTION

Synthetic aperture radar (SAR) holds some advantages against optical image acquisition. SAR is an active system, which can operate during day and night. It is also weather-independent and during bad weather conditions, SAR is the only operational system. Road extraction from SAR images therefore offers a suitable complement or alternative to road extraction from optical images. With the recent development of new high resolution SAR-systems, automatic road extraction faces new challenges. Satellite SAR images up to 1 m resolution will be available in 2006 by the German satellite TerraSAR-X [Roth, 2003]. Airborne images already provide resolution up to 1 decimetre [Schimpf, et al., 2002]

Automatic road extraction from SAR imagery remains still a complicated task, due to the side-looking geometry and the speckle effect. Especially in urban or forest areas, roads are occluded by shadow and layover, caused by adjacent high buildings or other high objects. Furthermore, building structures, traffic signs and metallic objects in cities give rise to dominant scattering. The most prominent scatterers are double-bounce scattering caused by reflections between the front of a house and the ground and triple-bounce scattering at trihedral corner structures at buildings. Also side-lobes, due to specular reflections from house roofs or metallic structures, appear frequently in urban scenes. All these imaging effects occlude important road information and make automatic road extraction complicated.

Preliminary work has shown that fusion of a pair of SAR images each taken from perpendicular and anti-parallel views improves the extraction of urban road networks [Tupin, et al. 2002]. In this work, the extraction is made in two steps, first a line detector adapted to the speckle statistic is used and afterwards a network based on a Markovian approach is reconstructed. Two dense urban areas were chosen as test scenes. Both scenes are characterized by a regular road network

of mainly perpendicular crossroads. The proposed method favours this kind of road networks.

Road extraction is carried out in simulated multi-aspect SAR images of an urban scene in [Dell'Acqua et al., 2003]. A fusion strategy is proposed in this work, which favours longer road segments. The research shows that a combination of multiple SAR views improves the results.

That the illumination direction is of importance for the road visibility was confirmed by [Stilla et al., 2004]. Simulations of layover and shadow effects of a selected urban scene were carried out for a set of aspect and incidence angles. The conclusion of the work is that the best results for the visibility of roads were obtained, when the illumination direction coincide with the main road orientations.

In this paper, an approach for fusing extracted road networks from multi-aspect SAR images, with special regard on SAR specific features is presented. First we ascertain good visibility conditions to build up rules for fusion strategy. Then, in the fusion part, each road segment is evaluated according to the rules for SAR images. While good candidates for road segments are kept, poor candidates, possible false alarms, are avoided. Our approach is based on the automatic road extraction system developed for rural areas [Wessel et al., 2003], [Wiedemann et al., 1999].

Images of a sub-urban scene recorded with different aspect angles for an improved extraction are analyzed in this work. In Section 2 we explain in detail the visibility aspects of roads in SAR images, with special focus on illumination problems (layover and shadow) of objects beneath the road. Section 3 contains a presentation of the road extraction performance, which focuses on the fusion of multi-aspect SAR images. In the end, the results of road extraction from single and multiple views are discussed.

2. ROAD VISIBILITY ANALYSIS

In contrast to optical images, roads in SAR images appear as dark lines. The smooth surface of the road, behaves like a mirror, which totally reflects the signal. This leads to a low signal and a homogeneous appearance of the road.

Much effort has been put on a statistical correct treatment of the speckle effect. But in the same way the effects caused by the side-looking geometry of SAR, layover and shadow, are relevant for radar images for urban as well as for rural scenes. These effects and their influence on the visibility of the road, with the emphasis of the aspect angle will be discussed further in this section.

2.1 Shadow and layover-effects

Shadow and layover effects are present at steep surfaces and depend on the incidence angle (off-nadir angle θ), the height of the target (h) and the slope of the target surface. Let us assume a row of high trees adjacent along one side of the road. When the illumination comes from the side, the trees cause a long often homogenous shadow, which partly cover the road. In Figure 1a, the length of the shadow s of one of the trees is depicted. The length of the layover l and the length of the shadow s is given by

$$l = h \cdot \cot(\theta), \quad (1)$$

$$s = h \cdot \tan(\theta). \quad (2)$$

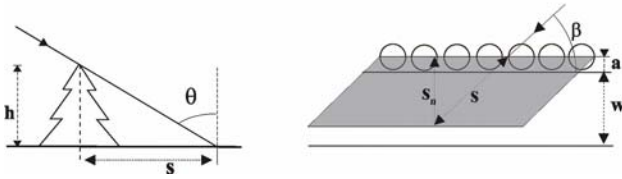


Figure 1: Shadow length of a row of trees a) Side view b) View from above

The shadow effects caused by the trees vary with the direction of the road in relation to the position of the SAR sensor. The layover- and shadow lengths perpendicular to the road (l_n , s_n) can be expressed as

$$l_n = h \cot(\theta) \sin(\beta), \quad (3)$$

$$s_n = h \tan(\theta) \sin(\beta), \quad (4)$$

where β is the angle between the range direction and the direction of the road. In this work, β is called the road visibility angle.

2.2 Shadow aspects

By automatic road extraction, one problem is to differentiate between true roads and long homogenous shadow areas, which have a similar appearance as roads. These shadow areas are often caused by the outer edge of a forest area, by a row of high trees or by high buildings. The problem is to differentiate between a false and a true road segment. However, the closer the orientation of the road segment to the range direction is (i.e.

when β approaches 0°), the higher is the possibility that the road segment is a true candidate.

For differentiation between road-like shadows parts and roads we take the line structure of the roads in account. Lines have two parallel, locally straight edges. When high objects are located at both sides of the road, the line structure is hard to be present even for roads with very small road visibility angles. In forest areas, tree branches bending over the road give the road an irregular shape.

When high objects are adjacent at one side of the road, the situation looks different. For a road with a width (w) of about 8 m bordered by 10 m high trees, standing 2 m away from the road (a), the road is detectable for road visibility angles below 40° ($\theta \approx 45^\circ$), according to Equation 3-4. A maximum road visibility angle, β_{max} , is introduced;

$$w + a > s_n \rightarrow \sin(\beta_{max}) < \frac{w + a}{h \tan(\theta)} \quad (5)$$

The nadir angle θ varies with near, middle and far range. It is therefore necessary to take this variation in consideration. The local incidence angle is

$$\tan(\theta) = \frac{D_{GR}}{H}, \quad (6)$$

where H is the flight attitude and D_{GR} is the ground range distance.

3. ROAD EXTRACTION AND FUSION OF MULTIPLE SAR VIEWS

In this chapter, the automatic road extraction for multiple SAR views will be described. First the general road extraction approach will be described briefly. Afterwards the focus will be on the fusion algorithm and its application for multiple SAR views.

3.1 Extraction of roads from single SAR views

The extraction of roads from SAR images is performed with the TUM road extraction approach [Wessel et al., 2003], which was originally designed for optical images with a ground pixel size of about 2m [Wiedemann et al., 1999]. The workflow of the extraction procedure is illustrated in Figure 2. The first step consists of line extraction using Steger's differential geometry approach [Steger, 1998]. Results from the line extraction step are shown in Figure 3. By applying explicit knowledge about roads, the line segments are evaluated according to their width, length, curvature, etc (see Figure 4). The evaluation is visualised in different colours on the principle of a traffic light. Green responds to "good road candidates", whereas red represents the worst candidates. A weighted graph of evaluated road segments is constructed. For the extraction of the roads from the graph supplementary road segments are introduced and seed points are defined. In our case, best-valued road segments serve as seed points. They are connected by an optimal path search through the graph. The roads extracted from one single view are presented together with the fusion results in Chapter 4 (Figure 7a-b).

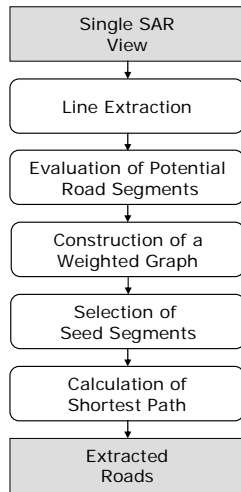


Figure 2: The workflow of the automatic road extraction procedure

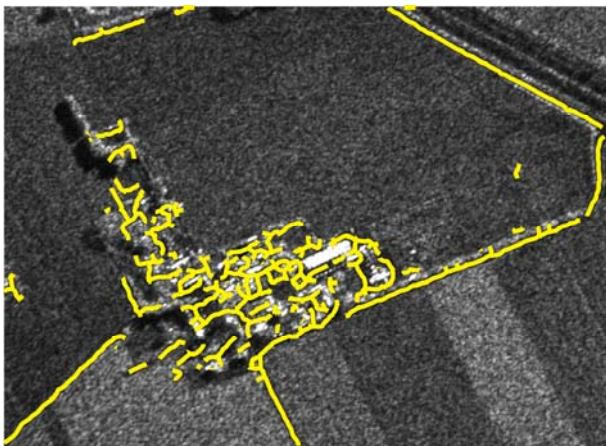


Figure 3: Line extraction results

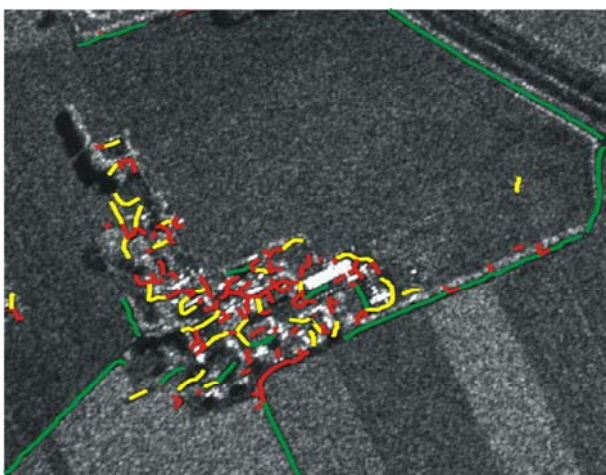


Figure 4: Evaluation of road segments

3.2 Fusion of extracted roads

Dealing with more than one image, we have to find a strategy for the fusion in order to keep the best-evaluated road segments. In our approach we analyse each image separately and implement the fusion first at the end of the process. A workflow of the procedure is illustrated in Figure 5.

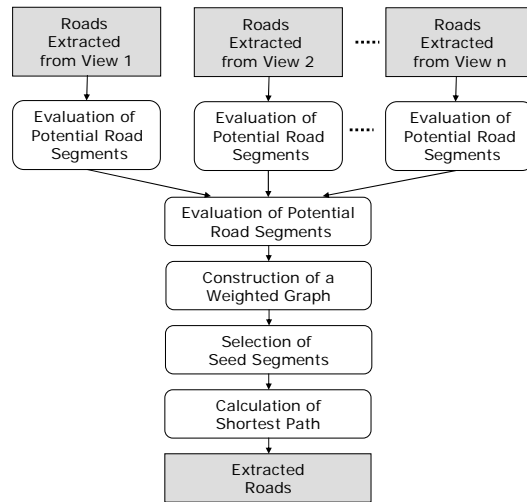


Figure 5: The workflow illustrates the fusion process of roads extracted in single views.

The roads extracted in each single image are fused together by the following iterative fusion strategy. Each road is split into segments and each segment is evaluated with respect to its road visibility angle. All segments are sorted according to its weight. The best-evaluated segment is chosen first and is added to the final result without any modification. Then, all neighbouring segments are searched for. Those parts of the neighbouring segments, which satisfy overlap and collinearity criteria (i.e. buffer width and direction difference) are assumed to be redundant extractions and are removed. The best-evaluated segment is divided into not-fused and fused parts to give the overlapping parts different weights compared to the non-overlapping parts, thereby accommodating the support provided by the redundant segments. Non-overlapping segments keep their previous evaluation. Also, lines with an all too deviant direction according to the best-evaluated line remain in its original state.

Then, the segment yielding the second highest evaluation is chosen and processed with the same algorithm. The whole fusion process ends after all segments have been processed. Finally, intersections are generated by checking for segments crossing each other. A fusion example is illustrated in Figure 6.

Fusion can be implemented in the beginning, middle or in the end of the extraction process. In our case, both fusion of conclusive extraction results at the end and fusion of road segments at an early stage, after the fuzzy evaluation, have been performed. Unfortunately this showed weak results due to two main reasons. Short small line segments extracted in forest areas or settlement areas, were in unfavourable cases detected in several image and therefore obtained a high evaluation. By fusion at the end, these poor candidates are already sorted out. The other reason is the “cutting” of the segments in the fusion process. By fusing at an early stage, seed points of a sufficient length are hard to obtain.

Finally a new road network based on the best-evaluated road segments (i.e. seed points) is generated. Only road segments that fulfil the following criteria are chosen as candidates for seed points:

- a road segment has to be detected at least twice
- or

- the direction of a road segment is within β_{max} (see Equation 5)
- and
- the length of the road segment should increase a given length.

These rules guarantee correct seed points with high evidence for roads based on the knowledge of the imaging geometry and by the use of multiple SAR views.

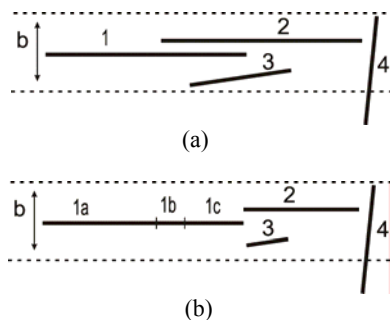


Figure 6: “Best-first” fusion a) Input: Line 1, 2, etc. are evaluated as best, second-best and third-best, respectively. b) Output: 1c is highest evaluated, while three lines are fused together; remaining parts of 1 (1a), 2 and 3 keep their evaluation. Line 4 is not even considered due to its deviant direction with respect to line 1. The next step would be to fuse line 2 and 3. The buffer-width b is marked out in the figure.

The results of the road extraction can afterwards be compared to reference data. The extracted data is matched to the reference data using a “buffer width”, similar to the one described above. Two quality measurements are applied:

Completeness is defined as the percentage of the reference data, which was detected during road extraction,

$$\text{completeness} = \frac{\text{length of matched reference}}{\text{length of reference}} \quad (4)$$

Correctness represents the percentage of the extracted road data, which is correct,

$$\text{correctness} = \frac{\text{length of matched extraction}}{\text{length of extraction}} \quad (5)$$

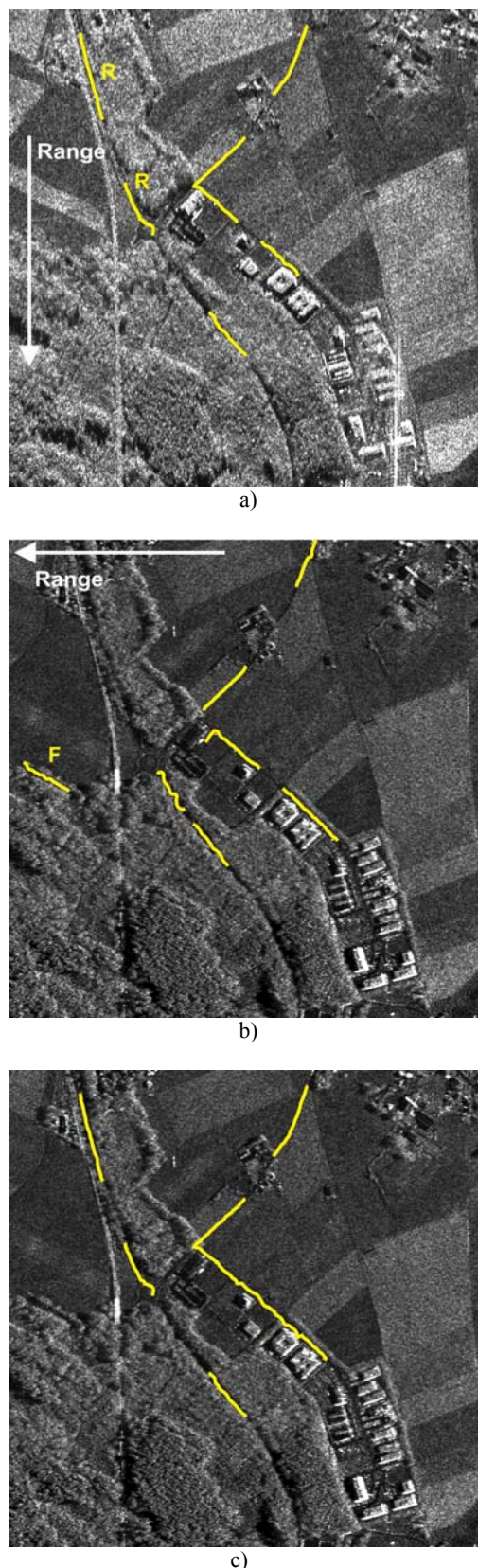


Figure 7: SAR scene 1 single views: a) is viewed from the top ($\theta \approx 35^\circ$), b) is viewed from the right ($\theta \approx 50^\circ$), c) Results after fusion of a-c.

4. RESULTS

The proposed fusion approach is tested on X-band, multilook SAR data with a resolution of about 0.75 m. The test area is located near the airport of DLR in Oberpfaffenhofen, southern Germany. Two test scenes are chosen. Scene 1 is illuminated from two aspect angles, 0° and 90° . Scene 2 is illuminated from three different aspect angles 0° , 45° and 90° . The ground range SAR data was manually registered. The roads extracted in each single view and the results after fusion can be seen in Figure 7 and 8.

From the analysis of both scenes the same conclusion can be drawn. The results after fusion is more complete (more roads are extracted) and correct (i. e, less false alarms occur) than the result extracted in each single image. False alarms are marked by "F" and roads with a favourable direction (within β_{max}) are marked by "R".

Remarkable by the evaluation are the difference between the results of completeness, correctness and RMS of Scene 1a and Scene 1b in Table 1. The explanation is that manually extracted data from Scene 1a is used as a reference. Since the reference and the extracted data is obtained from the same image, Scene 1a obtained a high evaluation. The poor results of View 1b and

the fusion results are mainly due to registration error and manual extraction error. In forest areas, often shadows instead of roads are extracted. The accurate location of roads is hard to define and there are some discrepancy between the extracted road and their real position. Since the images are illuminated from perpendicular directions, the shadow areas are displaced from each other with several meters.

	Completeness	Correctness	RMS
View 1a	44.8 %	95.7 %	2.18
View 1b	29.7 %	66.5 %	5.18
Fusion of 1a and 1b	51.8 %	93.8 %	3.22

Table 1: Comparison of automatic extracted data to manual extracted reference data

By the analysis of scene 2, a road, which matches the road analysed in Section 2, can be found in the middle of the scene (marked by "+" in Figure 8b). Trees are located at the upper side of the road. In one image (Figure 8a), the road is occluded by shadow and in the other image (Figure 8c), the road is occluded by layover. The road is only visible in one of the images and due to its favourable direction the road is highly evaluated and remains in the final result.

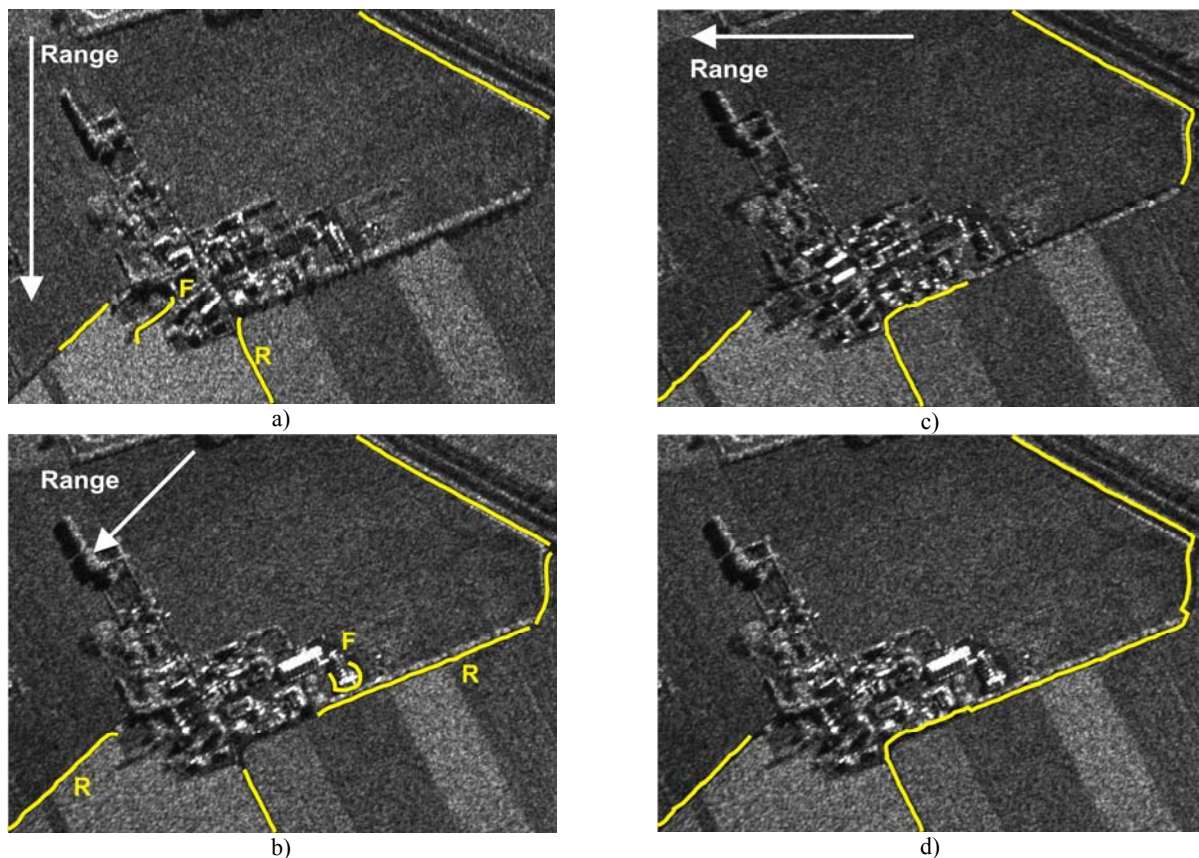


Figure 8: SAR scene 2 single view: a) is viewed from the top ($\theta \approx 51^\circ$), b) is viewed from the upper right corner ($\theta \approx 53^\circ$), c) is viewed from the right ($\theta \approx 52^\circ$), d) Fusion of a-c

5. OUTLOOK

In this article, we have presented a method for fusing road extraction results for multi-aspect SAR images. We managed a fusion strategy, which is based on selecting the best road candidate according to a visibility analysis. Regarding just road extraction by using multiple views, the conclusion can be made that not only the completeness of the road extraction is improved; also the correctness reaches a higher value by fusion of multiple SAR views. In any case, this analysis showed the capability of the “quality-ensuring” of the objects from a geometrical point of view. This assessment on object level is just a first step towards evaluation and can be performed in more sophisticated ways, based on fuzzy-values, statistics, etc. In future improvements, we will introduce a more sophisticated assessment.

Until now, we have not considered fusion of anti-parallel views. This is of particular interest, since an exposure of anti-parallel views involves less effort, than for example the exposure of perpendicular views. During the return flight, the scene can easily be illuminated a second time, but this time from the opposite direction. Figure 9 shows two anti-parallel SAR views of a rural area close to Ravensburg, Germany. The secondary road, which ranges from the top to the bottom of the scene, is partly covered in one image, but this part is visible in the other image and vice versa. The problems of fusing the extracted roads from two anti-parallel views are the “displacement” and the “gaps” of partly occluded roads or roads covered by shadows. Another step of future research will be to investigate the extraction and fusion of anti-parallel SAR views.

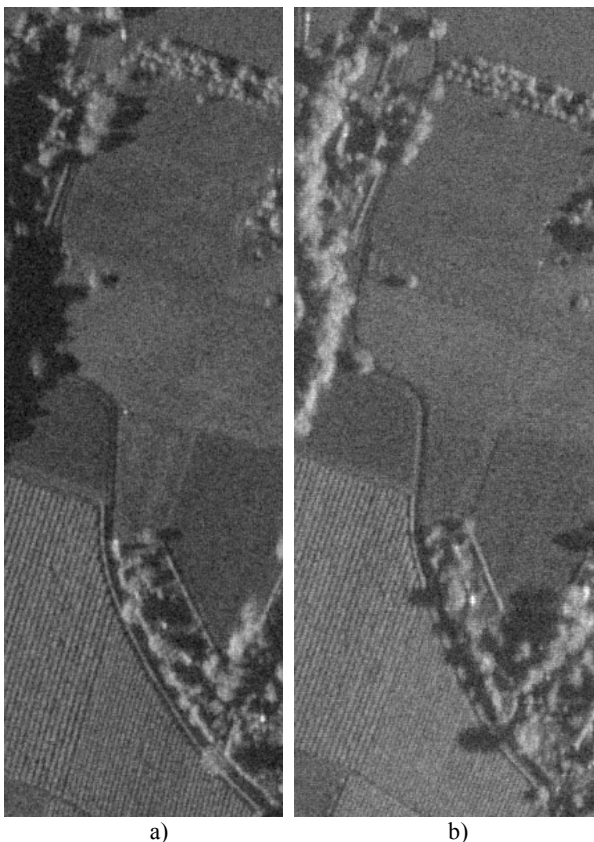


Figure 9: Anti-parallel SAR-views. a) illuminated from the left, b) illuminated from the right (MEMPHIS, 35GHz, resolution of 1m, $\theta \approx 60^\circ$, ©FGAN-FHR)

6. ACKNOWLEDGEMENTS

The authors would like to thank the Microwaves and Radar Institute, German Aerospace Center (DLR) for providing the SAR data of Oberpfaffenhofen.

We are also grateful to Dr. Essen and Mr. Haegelen at Research Institute for High Frequency Physics and Radar Techniques (FHR), Forschungsgesellschaft für Angewandte Naturwissenschaften e.V. (FGAN) for supplying the SAR data of Ravensburg.

This work was done within the TUM-DLR Joint Research Lab (JRL) [<http://www.ipk.bv.tum.de/jrl>], which is funded by Helmholtz Gemeinschaft.

REFERENCES

- Dell'Acqua, F., Gamba, P., Lisini, G. (2003) Improvements to Urban Area Characterization Using Multitemporal and Multiangle SAR Images. *IEEE Transactions on Geoscience and Remote Sensing*, 41(9), pp. 1996-2004
- Roth, A. (2003) TerraSAR-X: A new perspective for scientific use of high resolution spaceborne SAR data. 2nd GRSS/ISPRS Joint workshop on remote sensing and data fusion on urban areas, URBAN 2003. IEEE, pp. 4-7.
- Schimpf, H., Essen, H., Boehmsdorff, S., Brehm, T. (2002) MEMPHIS – A Fully Polarimetric Experimental Radar. *Geoscience and Remote Sensing Symposium*, 2002. IGARSS '02, Vol. 3, pp. 1714- 1716
- Soergel, U., Thoennessen, U., Stilla, U. (2003) Visibility analysis of man-made objects in SAR images. 2nd GRSS/ISPRS Joint workshop on remote sensing and data fusion on urban areas, URBAN 2003. IEEE, pp. 120-124
- Steger, C. (1998) An unbiased detector of curvilinear structures, *IEEE Trans. Pattern Anal. Machine Intell.*, 20(2), pp. 549-556
- Stilla, U., Michaelsen, E., Soergel, U., Hinz, S., Ender, H.J. (2004) Airborne Monitoring of vehicle activity in urban areas. In: Altan MO (ed) *International Archives of Photogrammetry and Remote Sensing*, 35(B3), pp. 973-979
- Tupin, F., Houshmand, B., Datcu, M. (2002) Road Detection in Dense Urban Areas Using SAR Imagery and the Usefulness of Multiple Views, *IEEE Transactions on Geoscience and Remote Sensing*, 40(11), pp. 2405-2414
- Wessel, B., Wiedemann, C. (2003) Analysis of Automatic Road Extraction Results from Airborne SAR Imagery. In: *Proceedings of the ISPRS Conference "Photogrammetric Image Analysis" (PIA'03)*, International Archives of the Photogrammetry, Remote Sensing and Spatial Information Sciences, Munich 2003, 34(3/W8), pp. 105-110
- Wiedemann, C., Hinz, S. (1999) Automatic extraction and evaluation of road networks from satellite imagery, *International Archives of Photogrammetry and Remote Sensing*, 32(3-2W5), pp. 95-100
- Wiedemann, C. (2001) *Extraktion von Straßennetzen aus optischen Satellitenbilddaten*, Dissertation